BROADBAND CHARACTERIZATION OF INDOOR POWERLINE CHANNEL

Er Liu, Yangpo Gao, Osama Bilal and Timo Korhonen

Communications Laboratory,
Helsinki University of Technology
Otaakari 5, Espoo, 02150, Finland
Phone: +358-9-4515671, Fax: +358-9-4512345
E-mail: {liuer, gyp, osama} @cc.hut.fi, Timo.korhonen@hut.fi

Abstract

For data communication over any medium, it is necessary to determine the characteristics of the communication channel. Powerline channel has been considered as a medium not only for low-rate, control purpose communication, but also for high-speed data communication, such as home networking and Internet access. In order to implement advanced communication technologies, the complete knowledge of the broadband powerline channel is required. This paper strives to widen understanding of broadband indoor powerline channel. We study the properties of mains cable and indoor PLC channel via their scattering parameters (S-parameters). Also, noise and interference of a PLC channel are measured in frequency domain.

1. Introduction

Powerline communication (PLC) has undergone a rapid development during recent years due to its promise of significant cost savings and versatility both in control and in general purpose data communication applications as in Internet distribution and in home networking. PLC channel shares some similarity to other wired media such as telephone local loop and Ethernet channels, still it has many significant differences, as its generally much larger interference and noise levels. Understanding of complete characteristics of broadband PLC channel is important when implementing advanced communication systems by using discrete multi-tone modulation (DMT) for channel capacity maximization [1].

Earlier research has been mainly focused on the frequencies below 30 MHz [2]. In this paper, our measurements extend from 0.1 MHz to 100 MHz, which is generally interesting for potential low spectral density, overlay-type PLC networking, and for high-speed networking in some countries. We study some key factors of PLC indoor channel, as its S-parameters, interference and noise behavior.

2. Measurement environment and devices

All the shown results are measured in a laboratory environment. Ballmann S200 network analyzer is used for S-parameters measurements, and R&S SRA spectrum analyzer is used to measure the noise and interference in frequency domain with a resolution of 50 kHz.

A coupling circuit [3] is used as an interface between powerline and measurement devices. We apply a custom designed broadband coupling circuit that provides high-pass type galvanic isolation between mains and measurement equipment. Our design, shown in figure 1-1, allows transmitting and receiving high frequency signal and blocks the 50 Hz mains. The coupling circuit is composed of a broadband 1:1 transformer and polyester capacitors, combination of which acts as a highpass (LC) filter. In the secondary stage of the transformer, five 1N4148 switching diodes clamp the output voltage of the coupling circuit, thus protecting the sensitive measurement equipment. If there is a voltage spike larger than 2.1V across the output, diodes D1, D3, D4 will turn on and clamp the output voltage. Conversely, if the voltage spike is less than –2.1V, diodes D2, D3, D5 will turn on and clamp the output voltage.

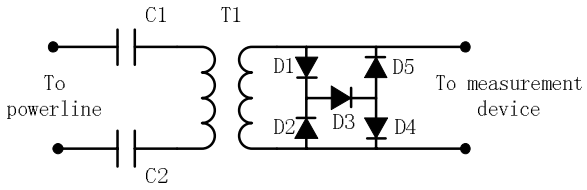

Figure 1-1. The coupling circuit.

Calibration of the coupling circuit is done before the measurements enabling exclusion of its effect from the channel measurement data.

3. S-parameters of indoor powerline channel

3.1 Measurement of mains cables

In Finland, a typical indoor mains cable has two or three conductors, whose cross section is depicted in Figure 3-1 [4]. The most common insulation material of low voltage power cables is polyvinyl chloride (PVC). When a higher temperature grading is needed, polyethylene or rubber is used in the power cables as the

insulation material. The insulation materials and conductor materials have a significant role in determining the high frequency characteristics of the power cables. However, it is not practical to define any general dielectric characteristics of PVC, because they depend heavily on the factors like temperature, frequency and the exact composition of the insulation material. Figure 3-2 shows the relationship between relative dielectric constant, frequency, and temperature.

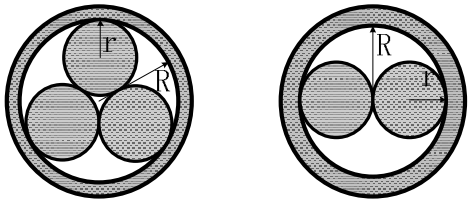

Figure 3-1. Cross sections of a typical indoor cables.

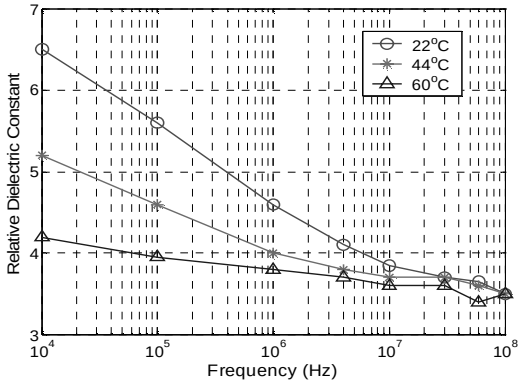

Figure 3-2 Relationship of the relative dielectric constant, frequency and temperature [4].

Due to the non-ideality of the conductors and insulation materials, part of the power that the transmitter injects into the cable does not reach the receiver. The main loss mechanisms of low voltage (220 V) power cables at the signal frequencies (as applied recently up to 30 MHz) used in power-line communications are the dielectric losses, resistive losses and coupling losses [4]. According to the transmission line theory [2], a small piece of PLC cable can be modeled mathematically by its distributed parameters R, C, L, and / or G:

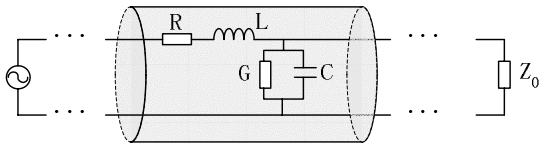

Figure 3-3. A distributed transmission line model.

When feeding signal into the two conductors, most of the electric field is concentrated between these two conductors. Considering the frequency in MHz range [5], the resistance per unit length is dominated by the skin effect. R and G vary as a function of frequency by

$$R \propto \sqrt{f}\ ,\ G \propto f. \tag{1}$$

Z_L, the characteristic impedance, and γ the propagation constant, can be expressed by

$$Z_L = \sqrt{Z/Y} = \sqrt{\frac{R + j\omega L}{G + j\omega C}} \tag{2}$$

$$\gamma = \sqrt{(R + j\omega L)(G + j\omega C)} = \alpha + j\beta. \tag{3}$$

In a real transmission line, attenuation caused by R and G is much less than by L and C, i.e. $R \ll \omega L$ and $G \ll \omega C$ yielding a simplification

$$Z_L = \sqrt{\frac{L}{C}} \tag{4}$$

$$\alpha = \frac{R}{2}\sqrt{\frac{C}{L}} + \frac{G}{2}\sqrt{\frac{L}{C}} = \frac{R}{2}\frac{1}{Z_L} + \frac{G}{2}Z_L \tag{5}$$

$$\gamma = k_1\sqrt{f} + k_2\sqrt{f} + jk_3 f. \tag{6}$$

Here the real part of the propagation factor α is the attenuation loss, which is proportional to $\sqrt{f}$, or f, or the combination of both. Figure 3-4 shows the measured attenuation of a bundle of indoor mains cables with the length of 20 meters.

Cable Type	Size (mm^2)
Vulcanize rubber cable (three-wire)	0.75
Vulcanize rubber cable (three-wire)	1
PVC/PVC cable (three-wire)	0.75
PVC/PVC cable (two-wire)	0.5

Table 3-1. Types and sizes of the measured cables.

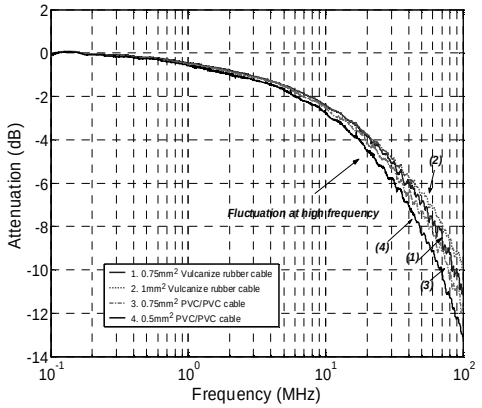

Figure 3-4. Attenuation of the mains cables.

Maximum of 4 dB attenuation difference among the mains cables is observed at 100 MHz. The rapid fluctuation at the ending of the curves is caused by impedance mismatching of the coupling circuit at higher frequencies.

3.2 PLC channel measurement

3.2.1 Channel transfer function (S_{21})

Channel measurements are taken between central switch and different sockets in our lab. Three different measured sockets are shown in Figure 3-5. The maximum distance between central switch to the sockets is 15 meters. Compared to 20 meters LOS path (single cable), the PLC channel is far from ideal. The deepest frequency notch is up to 23.2 dB lower than the ideal case. On average, 5-10 dB degradation is observed over the 100 MHz bandwidth.

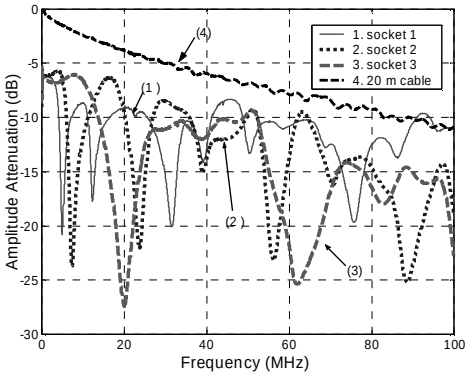

Figure 3-5. S_{21} parameters of different sockets.

Taking the socket 2 as an example, Figure 3-6 presents its frequency, phase and group delay responses in more details. This channel measurement verifies that, in general, attenuation increases gradually with the distance, as expected. PLC channel has obvious multipath and frequency selective fading phenomenon. The channel owns time varying characteristics also due to the various devices that are switched in/out and on/off in the powerline network.

Phase nonlinearities in the frequency response of the communications channel lead to variations in group delay, which disturbs data transmission. Phase response presents a "quasi" linear attribution decreasing as a function of frequency. Nonlinearities occur only in the frequency bands having a steep notch or a peak in the amplitude response. Impulse response of the channel can be found by IFFT transform of the measured transfer function (Fig. 3-6).

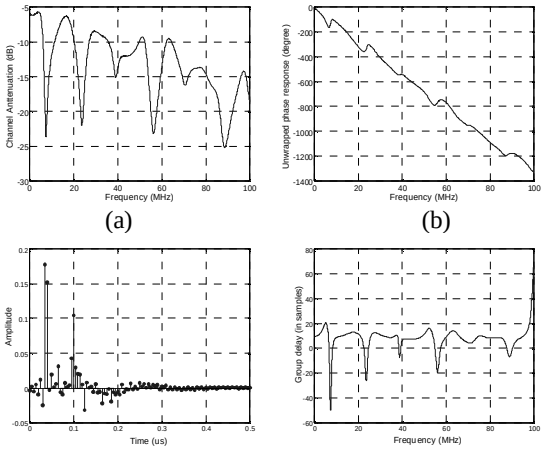

Figure 3-6. Channel measurements. (a) Frequency response, (b) Phase response, (c) Impulse response, (d) Group delay.

In this measurement, LOS path was about 11 meters, and it was followed by the two lower amplitude NLOS paths with the propagation distances of 30 m, and 37.5 m respectively. According to [5]'s powerline channel model, the weight of the different paths were 0.178, 0.105, and –0.025 respectively. To compensate this frequency selective fading in the wideband data transmission, some channel estimation and equalization methods are needed [6].

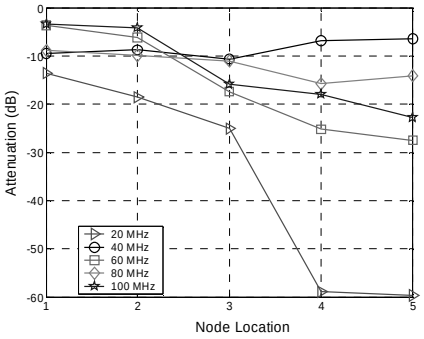

Figure 3-7. Attenuation of certain frequencies along the propagation path.

Figure 3-7 gives some frequencies' attenuation along the propagation path. In general, attenuation increases while the distance increases, but it does not follow strictly the trend that the higher the frequency, the larger the attenuation.

3.2.2 Reflection coefficient (S_{11}) and Network impedance

Impedance of a PLC-channel is dependent on the location of PLC-signal injection and its band of

frequencies. It is influenced by the characteristic impedance of the mains cable, topology of the network, and connected electrical loads. According to the statistical analysis [4] of the measurements performed for a few hundred in house powerline channels in the frequency band of 0 – 30 MHz, the average input impedance of the distribution network is between 100 ohms and 150 ohms. The impedance behavior can be directly obtained from S_{11} or S_{22} parameter by

$$S_{11} = \frac{Z_L - Z_o}{Z_L + Z_L}, \text{ So } Z_L = Z_o \frac{(1+S_{11})}{(1-S_{11})}. \quad (7)$$

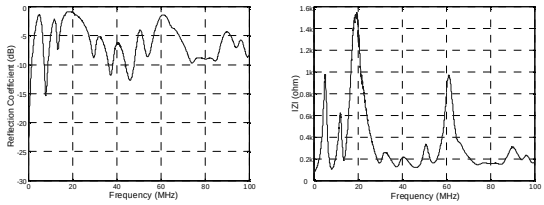

Figure 3-8. S_{11} parameter and the related impedance performance.

In our measurements, the impedance was strongly frequency variant, and discontinuous due to the of other network loads. The peak impedance may reach 1500 ohms, while on average, the network input impedance was around 200 ohms.

4. Interference and noise measurements

Besides signal attenuation and phase distortion, noise and interference are important factors that influence on the success of digital communications. In this section, we focus on the crosstalk of bundled mains cables as well as the noise analysis of a practical PLC-channel.

4.1 Crosstalk: FEXT and NEXT

A primary impairment of PLC-channels is the crosstalk from adjacent loop. Crosstalk manifests itself as an extra noise source introduced by the pairs within the same binder group. It has the two classifications: NEXT (Near-End crosstalk) and FEXT (Far-End crosstalk).

NEXT is defined as the crosstalk effect between a receiving path and a transmitting path of the transceivers at the same end of the two different cables within the same bundle. Figure 4-1 illustrates the formation of NEXT.

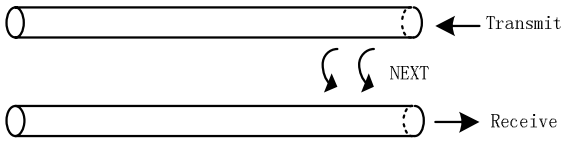

Figure 4-1. NEXT formation.

The NEXT transfer function $H_{NEXT}(f)$ can be approximated by using the 15-dB-per-decade model [7]. A typical NEXT-power transfer function $|H_{NEXT}(f)|^2$ shows then an $f^{2/3}$ characteristics:

$$|H_{NEXT}(f)|^2 = (N/49)^{0.6} \cdot 10^{-4} (d/km) \cdot (f/MHz)^{3/2}. \quad (8)$$

Here N is the number of interferers, and f is expressed in MHz. The NEXT loss $a_n(f)$ can be written as:

$$a_{next}(f) = 6 \cdot \log_{10}(N/49) - 40 + 15 \cdot \log_{10}(f/MHz). \quad (9)$$

In Fig. 4-2, a measured NEXT over powerline cable is compared to the 15-dB-per-decade model. It is obvious that the powerline channel has a smaller NEXT noise than the normal local loop phone line, since the powerline is a bus structure unlike the phone line, whose characteristics are comparably similar in different premises. The respective attenuation difference varies from 25dB to 40dB, approximately.

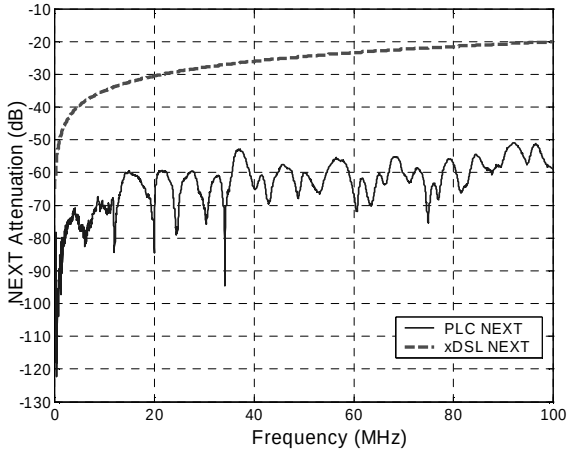

Figure 4-2. Powerline NEXT vs. 15-dB-per-decade model.

FEXT is defined as the crosstalk effect between a receiving path and a transmitting path of the transceivers at the opposite ends of the two different cables within the same bundle. Figure 4-3 illustrates the formation of FEXT.

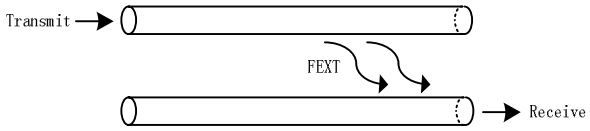

Figure 4-3. FEXT formation.

FEXT can be modeled by the 20-dB-per-decade model [7].

The FEXT-power transfer function $|H_{FEXT}(f)|^2$ shows an f^2 characteristics:

$$|H_{NEXT}(f)|^2 = (N/49)^{0.6} \cdot 3 \cdot 10^{-4} (d/km) \cdot (f/MHz)^2 \quad (10)$$

The model indicates, that the FEXT loss $a_{fext}(f)$ decreases while increasing the frequency by 20 dB per decade. The FEXT loss can be written as:

$$a_{fext}(f) = 6 \cdot \log_{10}(N/49) - 35 + 10 \cdot \log_{10}(d/km) + 20 \cdot \log_{10}(f/MHz). \quad (11)$$

Figure 4-4 shows a measured powerline FEXT noise compared to the 20-dB-per-decade model. We notice that, unlike in the NEXT case, PLC FEXT starts to decrease at the higher frequencies (60 MHz in our measurement). This is because FEXT signal will be attenuated along the full length of the transmission cable. So, the FEXT is a less severe transmission impairment than the NEXT. In order to study the length-independent property of FEXT, we define another concept called the Equal Level FEXT (ELFEXT), which adds the cable attenuation back in and removes the length dependency:

$$ELFEXT = FEXT - Cable\ Attenuation. \quad (12)$$

ELFEXT is more important for the systems that employ full duplex transmission. In Figure 4-4, the uppermost curve is the cable attenuation. The lowest curve is ELFEXT. The second curve refers to the 20-dB-per-decade model, and the third curve is the measured PLC FEXT signal.

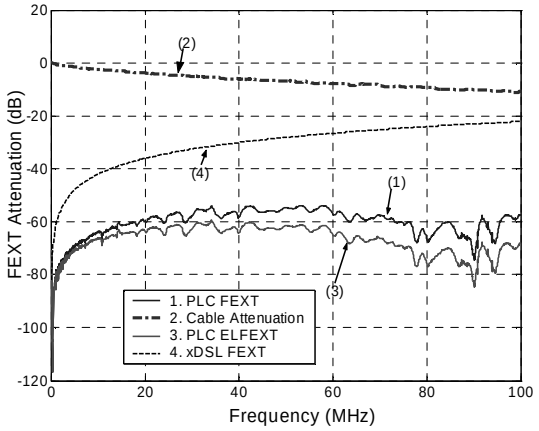

Figure 4-4. Powerline cable loss, FEXT and ELFEXT.

4.2 Noise measurements

Noise environment of a PLC network is very complex [8]. This noise can be classified into five categories:

1) Colored background noise
2) Narrow band noise
3) Periodic impulsive noise
4) Periodic noise
5) Asynchronous impulsive noise

Among these, the colored background noise and the asynchronous impulsive noise are the most important. Figure 4-5 shows a sample of colored background noise spectrum measured in our laboratory. We can see that the background noise is smoothly distributed over the spectrum. Its power spectral density is found to be a decreasing function of frequency, on average equal to

$$N(f) = 10^{a-b \cdot f^c} \text{ (W/Hz).} \quad (13)$$

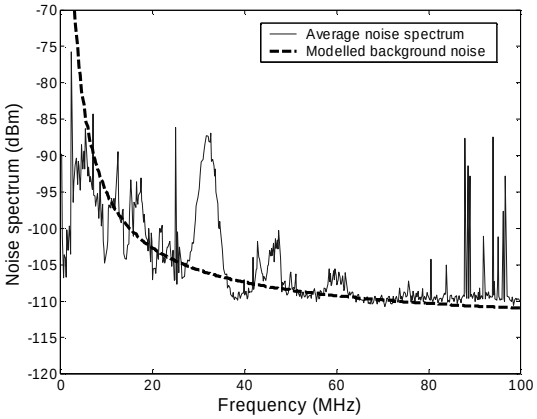

Figure 4-5. Background noise and its approximation.

By using the polynomial curve fitting algorithm provided by MATLAB, we find that $a = -115$, $b = 100$, and $c = -0.8$ that proves to be in a relatively good agreement with the measurement results as shown in the figure.

Asynchronous impulsive noise is caused by switching transients in the distribution network. The impulses have duration from some microseconds up to a few milliseconds.

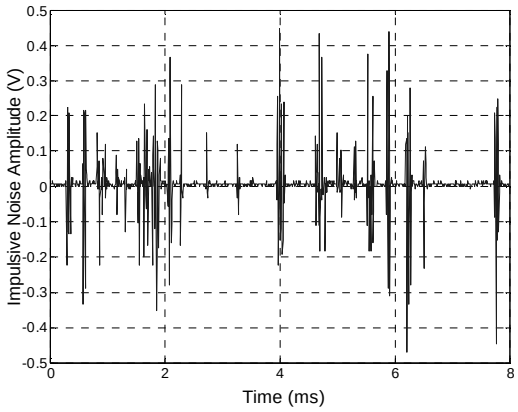

Figure 4-6. Asynchronous impulsive noise (in *ms* scale).

The power spectral density of this type of noise, on average, can have levels of 30 dB above the background noise. Figures 4-6 and 4-7 show typical asynchronous impulsive noise in the time interval of milliseconds and microseconds respectively.

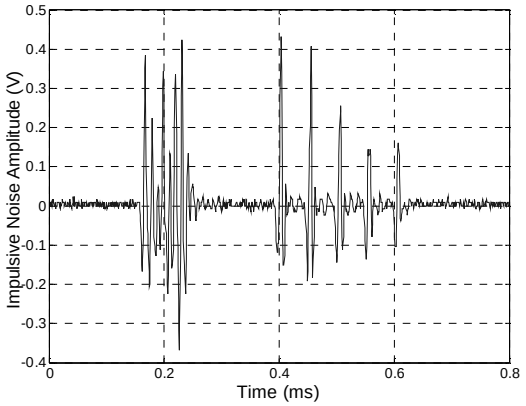

Figure 4-6. Asynchronous impulsive noise (in μs scale).

Amplitude, duration, and inter-arrival times are the three important properties used for modeling the impulsive noise. Based on 2000 measured samples, we found the statistical parameters indicated in Table 4-1.

Table 4-1 Statistical parameters of impulsive noise

	Mean	Standard deviation σ
Amplitude (mV)	229	121
Duration (μs)	205	157
Interval time (ms)	0.667	0.445

5. Conclusions

In this paper, we have carried out a survey of indoor powerline broadband characterization based on channel measurements. The measurement frequencies spanned up to 100 MHz, which is potentially applicable for future broadband overlay PLC applications, when the applied power levels are fitted to the specific EMC-regulations of the respective geographical regions. Channel responses were investigated both in time and frequency domain. Noise studies were summarized by finding the parameters of noise statistics. One potential PLC interference, the crosstalk between the bundled cables, was measured and compared to the xDSL reference model.

The statistical information we provided can be used for PLC-modem design and optimization in a simulated point-to-point communication environment. Further, this information can also be applied to optimize physical, link and network levels of future PLC-networks.

Acknowledgments

This project was financially supported by TEKES, the National Technology Agency of Finland.

References

[1] Esmailian T., *et.*, "A Discrete Multitone Power Line Communications System," IEEE trans. Acoustics, Speech, and Signal Processing, ICASSP '00. Proceedings. Vol. 5, pp. 2953 – 2956, June 2000.

[2] Manfred Z., Klaus D., "Analysis and Modeling of Impulsive Noise in Broad-band Powerline Communications," IEEE trans. Electromagnetic compatibility, Vol. 44, pp. 249-258, Feb. 2002.

[3] Bilal O., *et.*, "Designs of Broadband Coupling Circuits for PowerLine Communication," To be published on Proceedings of 7th ISPLC Proceedings, Apr. 2004.

[4] Jero A., "Applicability of Powerline Communications to Data Transfer of On-line Condition Monitoring of Electrical Drives," Doctor thesis, Lappeenranta University of Technology, ISBN 951-764-783-2.

[5] Manfred Z., Klaus D., "A Multi-path Signal Propagation Model for the Power Line Channel in the High Frequency Range," 3rd ISPLC proceedings, 1999.

[6] Gao Y., *et.*, "Channel Modeling and Modem Design for Broadband Powerline Communications," To be published on Proceedings of 7th ISPLC Proceedings, Apr. 2004.

[7] Ha K., Cha Y., Lee J., "xDSL Network Evolution Strategies to Minimize Crosstalk of FTTC-ADSL," 14th ISSLS, Apr. 2002.

[8] Jung, S., "A Channel Model for Power Line Communication in Home Network," Proceedings on the 15th CISL Winter workshop, Japan, Feb. 2002.